Stator Winding Temperature Estimation of IPMSM Based on a High-frequency Voltage Signal Injection

Hwigon Kim, Hyun-Sam Jung, and Seung-Ki Sul
Seoul National University
hwigon@eepel.snu.ac.kr

***Abstract*- An Interior Permanent Magnet Synchronous Machine, IPMSM, has been widely adopted as a traction motor of electric/hybrid vehicles because of high torque density and wide operating speed region. In the operation of IPMSM, a winding temperature should be monitored to maximize the operating area of IPMSM while avoiding winding insulation breakdown. This paper proposes a stator winding temperature estimation method of IPMSM by using high-frequency (HF) resistance at low operation speed. A relation between HF resistance and the stator winding temperature is analyzed and verified in an experimental setup where the stator winding temperatures and the magnet temperatures can be measured. Based on the relation, the stator temperature estimation method has been devised in this paper. Experimental results, including online estimation, show that the proposed method can be utilized to estimate the stator winding temperature.**

I. INTRODUCTION

An Interior Permanent Magnet Synchronous Machine, IPMSM, has widely been used as a traction motor of electric and hybrid vehicles in automotive industries for the last ten years because of high torque density and a wide operating speed range [1]. In motor drive, monitoring a winding temperature is necessary to prevent a winding insulation breakdown and maximize the motor operation area without the insulation problem [2-5]. Attaching temperature sensors to the stator winding is one of the options to monitor the winding temperature. However, it is not compatible with a mass-production system due to concern about cost and reliability. Therefore, non-invasive methods have been researched to estimate the stator winding temperature.

There are two methods to estimate the temperature. One is a method based on a thermal model [4, 6]. In this method, temperatures of each motor part, including stator winding, can be estimated by solving a preconstructed thermal model of a motor. However, extensive calibration and commissioning time are required due to the complexity of the thermal model. Moreover, the estimation accuracy is highly dependent on an operating environment such as a cooling system, and a mechanical geometry.

The other is based on an electrical model. In this method, a winding resistance variation depending on a stator winding temperature in (1) is used to estimate the stator temperature.

$$R_{sw}\left(T_{sw}\right)=R_{sw0}\left(1+\alpha_{cu}\left(T_{sw}-20^{o}C\right)\right). \quad (1)$$

In this equation, $R_{sw}(T_{sw})$ denotes a stator winding resistance at winding temperature, T_{sw}, where R_{sw0} and α_{cu} represent a stator winding temperature at room temperature 20 ºC, and a temperature coefficient of copper, 0.393 %/ºC.

Previous researches estimate the stator resistance in various methods. In [7], a certain amount of DC was injected to detect a resistance variation in the induction machine. This method had estimated the resistance accurately but would cause torque pulsation. High-frequency (HF) harmonics induced by Pulse Width Modulation, PWM, also could be utilized to estimate the winding temperature [3]. In this method, no additional signal was required, but high computation power was necessary. A phase of a HF impedance could be utilized to estimate the winding temperature by injecting voltage of carrier frequency [8]. In this method, the winding temperature was calculated without a burden of computation. However, the HF impedance phase had been affected not only by resistance but also by inductance. Because a HF inductance varies against a magnet temperature [1], estimation accuracy by the method in [8] would be influenced by magnet temperature variation.

In this paper, it is newly devised that the stator winding temperature is estimated by using a d-axis HF resistance in the rotor reference frame. The d-axis HF resistance can be obtained by a d-axis HF voltage signal injection in low operation speed where DC-link voltage has a margin for synthesizing voltage reference, including the injected voltage signal [1]. The proposed method results in much smaller torque ripple and speed ripple compared to the DC injection method. Also, by decoupling the HF inductances, the magnet temperature does not affect the winding temperature estimation, which makes the stator temperature estimation more accurate.

II. HF RESISTANCE AND THE STATOR TEMPERATURE

The equation (2) represents a model of IPMSM in the rotor reference frame. When a HF signal is injected, the model can be simplified as in (3) under the assumption that injected signal angular frequency, ω_h, is much higher than rotating angular speed, ω_r.

D-axis HF equivalent circuit of IPMSM can be represented as in Fig. 1 [1, 9]. In the figure, d-axis HF resistance contains winding resistance $R_{winding}$, stator core loss $R_{core|stator}$, rotor core loss $R_{core|rotor}$, and magnet loss R_{magnet}. The resistance can be modeled as (4).

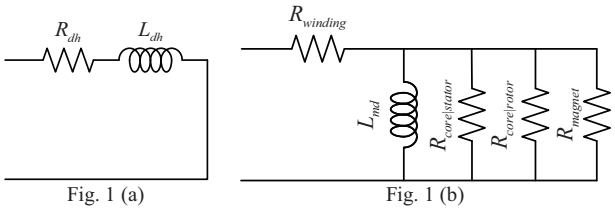

Fig. 1 (a) Fig. 1 (b)

Fig. 1 D-axis high-frequency circuit. (a) Series lumped equivalent circuit, and (b) d-axis high-frequency equivalent circuit.

$$\begin{bmatrix} v_{ds}^r \\ v_{qs}^r \end{bmatrix} = R_s \begin{bmatrix} i_{ds}^r \\ i_{qs}^r \end{bmatrix} + \begin{bmatrix} L_{ds} & L_{dqs} \\ L_{qds} & L_{qs} \end{bmatrix} p \begin{bmatrix} i_{ds}^r \\ i_{qs}^r \end{bmatrix} + \omega_r \begin{bmatrix} -L_{qs} & -L_{qds} \\ L_{dqs} & L_{ds} \end{bmatrix} \begin{bmatrix} i_{ds}^r \\ i_{qs}^r \end{bmatrix} + \omega_r \begin{bmatrix} \lambda_{pm} \\ 0 \end{bmatrix} \quad (2)$$

$$\begin{bmatrix} v_{dsh}^r \\ v_{qsh}^r \end{bmatrix} = \begin{bmatrix} R_{dh} + j\omega_h L_{dh} & j\omega_h L_{dqh} \\ j\omega_h L_{qdh} & R_{qh} + j\omega_h L_{qh} \end{bmatrix} \begin{bmatrix} i_{ds}^r \\ i_{qs}^r \end{bmatrix} \quad (3)$$

$$R_{dh} = R_{sw} + R_{core} + R_{magnet}. \quad (4)$$

The core loss varies according to the motor speed and load condition. Also, there are researches reported that magnet loss varies according to the magnet temperature [1, 10]. Therefore, the d-axis HF resistance can be denoted as (5), where T_e, ω, T_{sw}, and T_{mag} represent motor torque, speed, winding temperature, and magnet temperature, respectively. Here, the motor current is determined by torque.

$$R_{dh}(T_e, \omega, T_{sw}, T_{mag}) = R_{sw}(T_{sw}) + R_{core}(T_e, \omega) + R_{magnet}(T_{mag}). \quad (5)$$

The core losses and the magnet loss should be decoupled from a d-axis HF resistance to extract winding resistance and estimate the winding temperature. However, those losses are difficult to model theoretically. Therefore, in chapter IV, the effect of core loss and magnet loss will be disclosed experimentally.

III. Temperature Measurement System

A test setup has been developed to measure the IPMSM temperatures. Table 1 shows the parameter of IPMSM in use. Nine temperature sensors denoted as green dots in Fig. 2, are attached at each winding phase to measure the stator winding temperature. The magnet temperatures are measured at 32 different locations of magnets, denoted as black circles in Fig. 2. These magnet temperature sensors are directly attached to the magnets and rotate with the rotor, as shown in Fig. 3. The other board in the stationary part, which denoted as a yellow dashed line in Fig. 3, measure the stator winding temperature and transmit the temperature information to the control board. An error bound of the sensor is about ±1.1 ºC in the range from -50 ºC to 150 ºC. A detailed structure of the sensing system was described in [11].

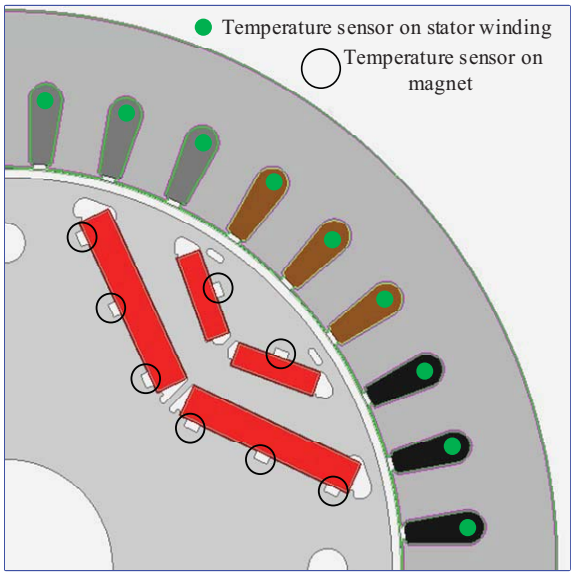

Fig. 2. Temperature sensor location on the winding and the magnet.

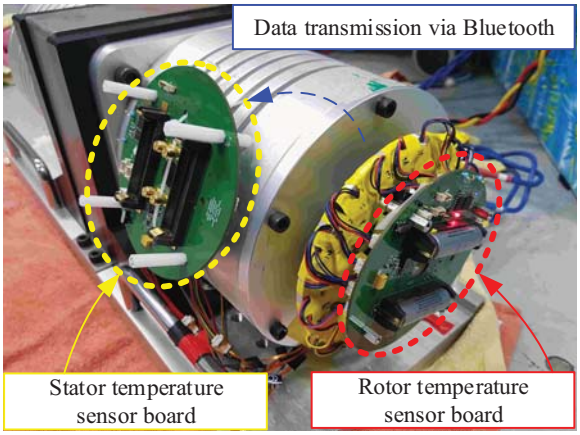

Fig. 3. Test motor with the temperature sensors.

Table 1: Parameters of IPMSM

Parameter	Value
Pole	4
Rated torque	10 N·m
Rated speed at 310V	1800 r/min
Magnet flux linkage	0.369 V·s

IV. Proposed Method and Experimental Results

A. D-axis HF Resistance Extraction

The d-axis HF resistance can be measured by injecting an additional HF voltage at d-axis. Fig. 4 shows the block diagram of the HF voltage signal injection method, where a HF voltage reference, v_{dqsh}^{r*} is added to the current controller output, v_{dqs}^{r*}. The HF voltage induces the HF current, which can be extracted by a bandpass filter, BPF, whose center frequency is the injection frequency.

Injected HF voltage can be represented as (6), where V_h is HF voltage magnitude, and ω_h is HF signal angular frequency.

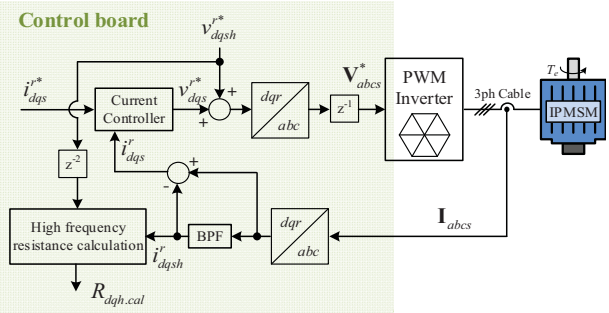

Fig. 4. Implementation of the HF voltage injection method.

HF voltage is injected only into the d-axis in the rotor reference frame to calculate the d-axis HF resistance.

$$\begin{bmatrix} v_{dsh}^{r} \\ v_{qsh}^{r} \end{bmatrix} = V_h \begin{bmatrix} \cos \omega_h t \\ 0 \end{bmatrix}. \tag{6}$$

Induced HF current can be represented as

$$\begin{bmatrix} i_{dsh}^{r} \\ i_{qsh}^{r} \end{bmatrix} = \begin{bmatrix} I_{dh} \cos\left(\omega_h t + \varphi_d\right) \\ I_{qh} \cos\left(\omega_h t + \varphi_q\right) \end{bmatrix}. \tag{7}$$

I_{xh} and φ_x represent induced HF current magnitude and phase, where x is a certain axis between d-axis and q-axis. Because of the cross-coupling effect, though HF voltage is injected in d-axis only, the HF current is induced both d-axis and q-axis.

From these equations, d-axis HF resistance R_{dh} is represented as follows.

$$R_{dh} = \frac{V_h}{I_{dh}} \cos \varphi_d. \tag{8}$$

φ_d and I_{dh} are calculated by demodulating injected HF voltage reference and induced HF current [12].

B. D-AXIS HF RESISTANCE AND THE STATOR WINDING TEMPERATURE

The HF resistance is measured at various torque, speed, magnet temperature, and stator winding temperature to demonstrate a relationship between a d-axis HF resistance and the stator winding temperature.

Rotating speed is swept from 300 r/min to 900 r/min with interval, 150 r/min. Torque is swept from 0 N·m to rated torque, 10 N·m, with 1 N·m interval. By heating the motor, winding temperature increases from 30 ºC to 75 ºC, and the magnet temperature increases up to 70 ºC with the winding temperature variation. After the winding temperature reaches 75 ºC, the motor is cooled down. While chilling, as the winding temperature decrease more rapidly than the magnet temperature, HF resistance can be measured in various winding and magnet temperature conditions.

Fig. 5 shows the relation between a d-axis HF resistance and the winding temperature at 900 r/min, 10 N·m. Because torque, that is, current and speed are fixed, and switching frequency is also constant, core loss would be a constant value. Therefore, the d-axis HF resistance equation in (5) varies only with stator winding temperature, and the magnet temperature.

Fig. 6 shows the magnet and the winding temperature at each measurement, where #n denotes nth measurement. Magnet temperatures differ by 15.4 ºC, while the stator winding temperatures are equals to about 60 ºC comparing 7th and 14th measurements. These points in Fig. 6 correspond to points denoted as #7 and #14 in Fig. 5. In these figures, despite the magnet temperature variation, measured d-axis HF resistances

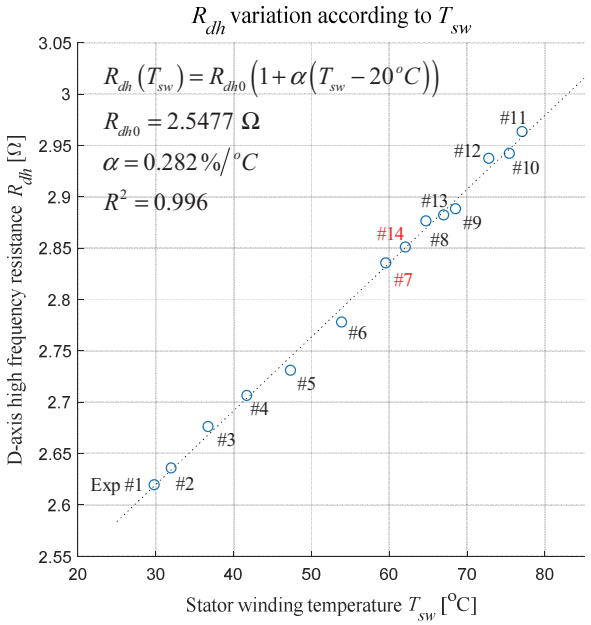

Fig. 5. Measured d-axis HF resistance.
R_{dh}: D-axis HF resistance. R_{dh0}: D-axis HF resistance when winding temperature 20 ºC. α: A temperature coefficient of d-axis HF resistance. R^2: Coefficient of determination of linear regression.

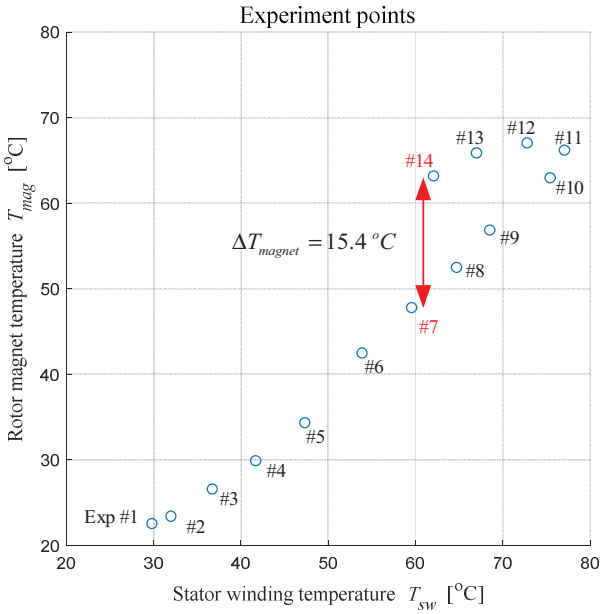

Fig. 6. Magnet and winding temperature at each experiment.
ΔT_{magnet}: Magnet temperature difference between 7th and 14th measurement.

coincide with the linear approximation between the d-axis HF resistance and the winding temperature. From this result, it can be said that a d-axis HF resistance hardly changed with the magnet temperature, and only varies with the winding temperature at a specific load condition. Since the magnet temperature does not affect d-axis HF resistance, (5) can be represented as (9), where the d-axis HF resistance modeled as a function of winding temperature only.

$$\begin{aligned} R_{dh}\left(T_{sw}\right)\big|_{T_e,\omega} &= R_{sw}\left(T_{sw}\right) + R_{core}\big|_{T_e,\omega} + R_{magnet} \\ &= R_{sw0}\left(1+\alpha_{cu}\left(T_{sw}-20\,^{\circ}\mathrm{C}\right)\right) + R_{core}\big|_{T_e,\omega} + R_{magnet} \\ &= R_{dh0}\big|_{T_e,\omega}\left(1+\frac{R_{sw0}}{R_{dh0}\big|_{T_e,\omega}}\alpha_{cu}\left(T_{sw}-20\,^{\circ}\mathrm{C}\right)\right) \\ &= R_{dh0}\big|_{T_e,\omega}\left(1+\alpha\big|_{T_e,\omega}\left(T_{sw}-20\,^{\circ}\mathrm{C}\right)\right). \end{aligned} \tag{9}$$

In Fig. 5, the relation between the winding temperature and d-axis HF resistance is highly linear with over 0.99 coefficient of determination [13]. A temperature coefficient of d-axis HF resistance, α, is 0.282 %/ºC, which is smaller than that of copper, 0.393 %/ºC. The reason for the smaller temperature coefficient is that α is decided with the ratio R_{dh0} and R_{sw0} as in (9).

The winding temperature is estimated by calculating a simple equation

$$T_{sw.estimate} = \frac{R_{dh.measure} - R_{dh0}}{\alpha} + 20\,^{\circ}\mathrm{C}. \tag{10}$$

From (10), which is an inverse form of (9), the maximum estimation error is 1.9 ºC from the experimental result in Fig. 5.

Fig. 7 shows the measured d-axis HF resistance at various speeds when load torque is 10 N·m. As in the figure, the linearity between the HF resistance and the winding temperature is held at every speed. Since the core loss increase as the speed increases, d-axis HF resistance is increased, and the temperature coefficient, α, is decreased.

V. Online Stator Temperature Estimation

To estimate the winding temperature, (10) can be adapted. However, estimated temperature using the equation includes noise because calculated d-axis HF resistance, $R_{dh.cal}$, from injected HF voltage as in Fig. 4 is noisy. Therefore, a simple temperature estimator is designed, as in Fig. 8. The estimator composed of a lookup table, a LUT, Eq. (9), and an integrator. From LUT, with torque and speed, α and R_{dh0} in (9) are obtained. With obtained constants and estimated winding temperature, $T_{sw.est}$, estimated d-axis HF resistance, $R_{dh.est}$, is calculated by (9). Then, the integrator output would be an estimated winding temperature.

By using the estimator, an online estimation is executed for 1600 seconds, as shown in Fig. 9. Stator winding temperature increases from 25 ºC to 75 ºC. Magnet temperature also increases from 25 ºC to 41 ºC. At 625 second, load torque is

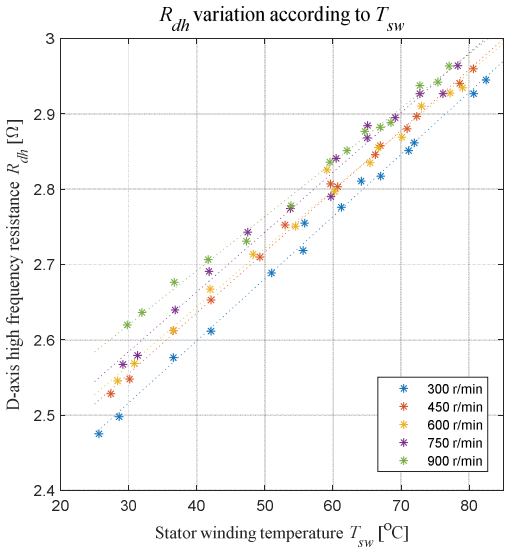

Fig. 7. The relation between d-axis HF resistance and winding temperature at various speed

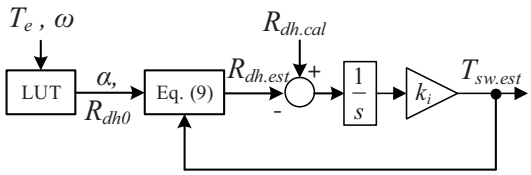

Fig. 8. A stator winding temperature estimator

reduced, and stator winding temperature decreases while the magnet temperature increase.

At various speed and torque, the winding temperature is estimated within maximum error 4 ºC, whether temperature increases or decreases. Also, it can be said that the estimation error caused by the magnet temperature variations can be negligible.

VI. Conclusion

In this paper, a stator winding temperature estimating method based on a d-axis HF resistance has been proposed. D-axis HF resistance is measured by HF voltage injection. A relation between the d-axis HF resistance and the winding temperature has been analyzed in the experimental setup that can measure the winding temperature and the magnet temperature, simultaneously.

By experimentally, elements that influence HF resistance have been analyzed, such as torque, speed, magnet temperature, and stator winding temperature. The d-axis HF resistance linearly increases as the winding temperature increases at various load conditions. By using the relationship, the winding temperature can be estimated in real-time within a maximum estimation of 4 ºC. Also, it is demonstrated that the proposed method is robust to the magnet temperature variation.

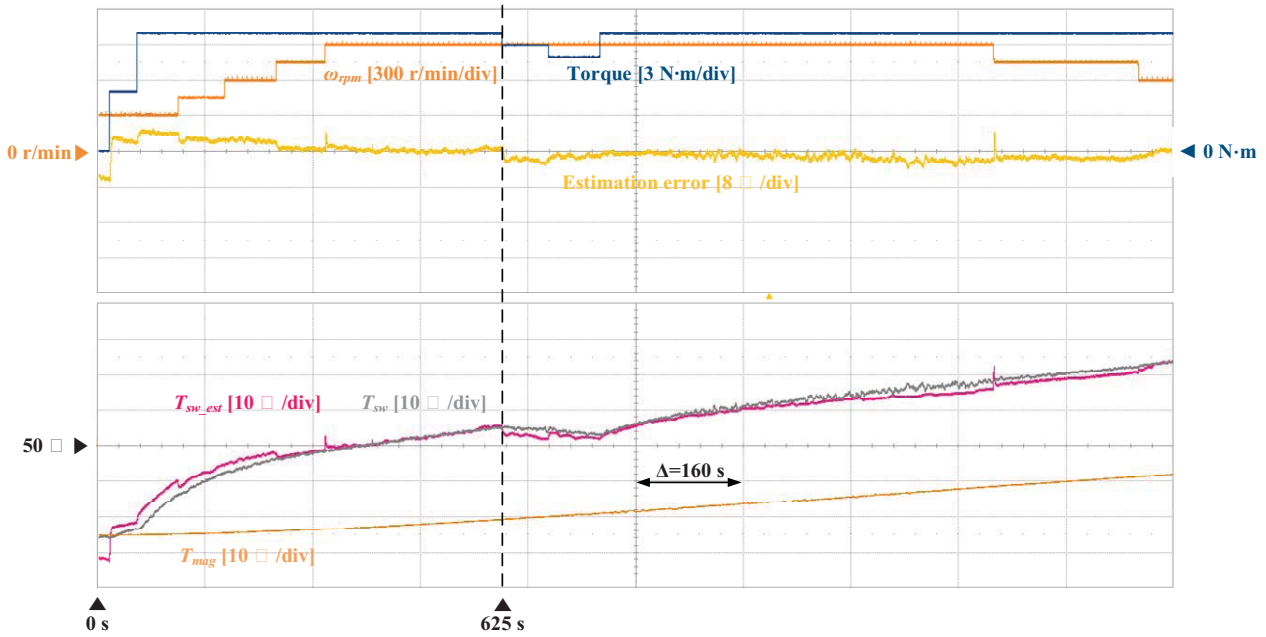

Fig. 9. Online estimation result. ω_{rpm} : motor speed, T_{sw_est} : estimated winding temperature, T_{sw} : stator winding temperature, T_{mag} : magnet temperature.

ACKNOWLEDGMENT

This work was supported by the Brain Korea 21 Plus Project in 2019-2020.

REFERENCES

[1] H. Jung, D. Park, H. Kim, S. Sul, and D. J. Berry, "Non-Invasive Magnet Temperature Estimation of IPMSM Based on High-Frequency Inductance With a Pulsating High-Frequency Voltage Signal Injection," *IEEE Transactions on Industry Applications,* vol. 55, no. 3, pp. 3076-3086, 2019

[2] L. He, S. Cheng, Y. Du, R. G. Harley, and T. G. Habetler, "Stator Temperature Estimation of Direct-Torque-Controlled Induction Machines via Active Flux or Torque Injection," *IEEE Transactions on Power Electronics,* vol. 30, no. 2, pp. 888-899, 2015

[3] N. Z. Popov, S. N. Vukosavic, and E. Levi, "Motor Temperature Monitoring Based on Impedance Estimation at PWM Frequencies," *IEEE Transactions on Energy Conversion,* vol. 29, no. 1, pp. 215-223, 2014

[4] C. Kral, A. Haumer, and S. B. Lee, "A Practical Thermal Model for the Estimation of Permanent Magnet and Stator Winding Temperatures," *IEEE Transactions on Power Electronics,* vol. 29, no. 1, pp. 455-464, 2014

[5] S. D. Wilson, P. Stewart, and B. P. Taylor, "Methods of Resistance Estimation in Permanent Magnet Synchronous Motors for Real-Time Thermal Management," *IEEE Transactions on Energy Conversion,* vol. 25, no. 3, pp. 698-707, 2010

[6] A. Boglietti, A. Cavagnino, D. Staton, M. Shanel, M. Mueller, and C. Mejuto, "Evolution and Modern Approaches for Thermal Analysis of Electrical Machines," *IEEE Transactions on Industrial Electronics,* vol. 56, no. 3, pp. 871-882, 2009

[7] L. Sang-Bin and T. G. Habetler, "An online stator winding resistance estimation technique for temperature monitoring of line-connected induction machines," *IEEE Transactions on Industry Applications,* vol. 39, no. 3, pp. 685-694, 2003

[8] F. Briz, M. W. Degner, J. M. Guerrero, and A. B. Diez, "Temperature Estimation in Inverter-Fed Machines Using High-Frequency Carrier Signal Injection," *IEEE Transactions on Industry Applications,* vol. 44, no. 3, pp. 799-808, 2008

[9] H. Jung, D. Park, H. Kim, S. Sul, and D. J. Berry, "Non-Invasive Magnet Temperature Estimation in IPMSM by High Frequency Pulsating Sinusoidal Voltage Injection," in *2018 IEEE Transportation Electrification Conference and Expo (ITEC)*, 13-15 June 2018 2018, pp. 858-862

[10] D. D. Reigosa, F. Briz, P. Garcia, J. M. Guerrero, and M. W. Degner, "Magnet Temperature Estimation in Surface PM Machines Using High-Frequency Signal Injection," *IEEE Transactions on Industry Applications,* vol. 46, no. 4, pp. 1468-1475, 2010

[11] D. Park, H. Jung, H. Cho, and S. Sul, "Design of Wireless Temperature Monitoring System for Measurement of Magnet Temperature of IPMSM," in *2018 IEEE Transportation Electrification Conference and Expo (ITEC)*, 13-15 June 2018 2018, pp. 656-661

[12] P. L. Jansen and R. D. Lorenz, "Transducerless position and velocity estimation in induction and salient AC machines," *IEEE Transactions on Industry Applications,* vol. 31, no. 2, pp. 240-247, 1995

[13] E. A. P. Douglas C. Montgomery, G. Geoffrey Vining, *Introduction to Linear Regression Analysis*, 5 ed. 2013, p. 688.